

## Role of Cholesterol and Polyunsaturated Chains in Lipid–Protein Interactions: Molecular Dynamics Simulation of Rhodopsin in a Realistic Membrane Environment

Michael C. Pitman,<sup>†</sup> Alan Grossfield,<sup>†</sup> Frank Suits,<sup>†</sup> and Scott E. Feller<sup>\*‡</sup>

IBM T. J. Watson Research Center, 1101 Kitchawan Road, P.O. Box 218, Yorktown Heights, New York 10598, and  
Department of Chemistry, Wabash College, 301 West Wabash Avenue, Crawfordsville, Indiana 47933

Received December 3, 2004; E-mail: fellers@wabash.edu

Biomembranes are highly complex, combining chemical heterogeneity and thermal disorder to produce structures whose physical properties vary widely over relatively small distances.<sup>1</sup> Unlike the simpler lipid bilayers often used in biophysical studies, biological membranes usually contain multiple lipid species, cholesterol, and integral membrane proteins. This complexity has biological importance; experiments suggest that organisms vary the lipid composition of their membranes to modulate protein function.<sup>2,3</sup> For example, the retinal rod outer segment disk membranes, which house the photoreceptor protein, rhodopsin are rich in polyunsaturated lipids and cholesterol, which modulate the rhodopsin photocycle.<sup>4,5</sup> Polyunsaturated lipids tend to congregate around proteins,<sup>6,7</sup> while cholesterol stabilizes rhodopsin and slows the kinetics of the photocycle,<sup>8,9</sup> but the structural and thermodynamic reasons for this behavior are not well understood at the molecular level. To address these issues, we present a 118-ns molecular dynamics simulation of rhodopsin embedded in a bilayer containing cholesterol and two different lipid species, each containing a polyunsaturated acyl chain. Although several notable rhodopsin simulations have been published recently,<sup>10–13</sup> the present work is unique due to its more realistic membrane composition and the time scale of the simulation, both of which are important for drawing biologically relevant conclusions. The simulation demonstrates that the protein breaks the lateral and transverse symmetry of the bilayer. Lipids near the protein preferentially reorient such that their unsaturated chains interact with the protein, while the distribution of cholesterol in the membrane complements the variations in rhodopsin's transverse profile. The latter phenomenon suggests a molecular-level mechanism for the experimental finding that cholesterol stabilizes the native dark-adapted state of rhodopsin without binding directly to the protein.<sup>14</sup>

The simulation contained a single rhodopsin molecule embedded in a bilayer composed of a 2:2:1 mixture of 1-stearoyl-2-docosahexaenoyl-phosphatidylcholine (SDPC), 1-stearoyl-2-docosahexaenoyl-phosphatidylethanolamine (SDPE), and cholesterol (1 protein, 49 SDPCs, 50 SDPEs, 24 sterols, and 7400 waters, for 43222 atoms in total). Each lipid contains a saturated 18-carbon chain (STEA) and a 22-carbon polyunsaturated chain (DHA). The membrane contains two different lipid headgroups, two acyl chain types, and 50 mol % polyunsaturated chains, which makes it a good, if simplified, model for a biological disk membrane. The resulting cholesterol concentration is comparable to that found in nature,<sup>5</sup> while the protein:lipid molar ratio is comparable to what is seen biologically and in model-membrane experiments.<sup>2,8,9</sup>

The bilayer system was built and equilibrated as described previously; the CHARMM27 force field was used throughout (see Supporting Information for further details on the system construction

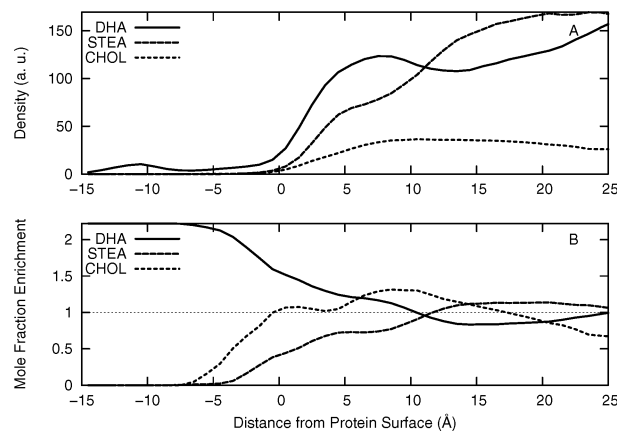


**Figure 1.** Distribution of membrane components, as a function of lateral distance to the protein, in Å. (A) Density of molecules in arbitrary units. (B) Ratio between the mole fraction for each component and its total mole fraction. “DHA” indicates the docosahexaenoyl chain, “STEA” the stearoyl chain, and “CHOL” cholesterol.

and simulation conditions).<sup>6,15–17</sup> Following equilibration, we ran a 118-ns trajectory in the NVE (constant particle number, system volume, and total energy) ensemble. The average system temperature was 311 K.

A number of major structural reorderings occurred during the early part of the simulation. For example, the cholesterol distribution around the protein evolved, and the C-terminal loop region, which was absent in the original crystal structure,<sup>18</sup> became disordered and then refolded. Furthermore, several water molecules entered the protein interior, binding in crystallographically significant regions.<sup>19</sup> Also during this time, several cholesterol molecules migrated between leaflets, with the result that the bulk of the simulation proceeded with 11 cholesterol molecules in the upper leaflet, 1 roughly in the center of the membrane, and 12 in the lower leaflet. We therefore excluded the first 20 ns of the trajectory and analyzed only the final 98 ns. During this part of the simulation, every lipid spent some time in contact with the protein. Given that cholesterol's lateral mobility is even greater than the surrounding lipid,<sup>20</sup> this suggests that the simulation was long enough to allow the membrane to sample a broad range of distinct configurations.

Experimentally, variations in lipid composition alter the thermodynamic stability and activation kinetics of rhodopsin.<sup>8,9</sup> The presence of multiple chain species in this system allows us to examine the details of this phenomenon with atomic resolution. Figure 1 shows the distribution of the three hydrophobic bilayer components as a function of the signed distance to the protein surface (see Supporting Information for details).

Figure 1A demonstrates that the protein is preferentially solvated by DHA. The finite probability for DHA to exist at negative

<sup>†</sup> IBM T. J. Watson Research Center.  
<sup>‡</sup> Wabash College.

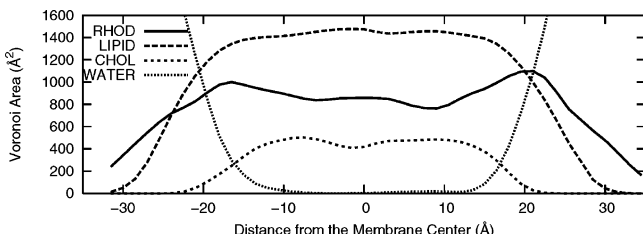


**Figure 2.** Voronoi areas for system components as a function of position along the membrane normal. “RHOD” indicates the protein, “CHOL” the cholesterol, and “WATER” the water. “LIPID” indicates the average of the areas for SDPC and SDPE.

distances from the surface is the result of a number of events where DHA chains penetrated between the helices; the other components did not significantly penetrate the protein surface. Figure 1B also indicates that the concentration of DHA is enriched near the protein, with a corresponding depletion of STEA. This agrees with previous experiments<sup>7</sup> and simulations<sup>6</sup> that concluded that rhodopsin is preferentially solvated by polyunsaturated lipid. By contrast, cholesterol redistributes near but not in contact with the protein. The mole fraction of cholesterol is enriched primarily in the region 5–15 Å from the protein surface, while the bulk of its short-range population is due to a pair of cholesterols that interact with the palmitoyl chains bound to Cys322 and Cys323. This distribution is consistent with experimental findings that suggest cholesterol stabilizes the native state of rhodopsin without binding to it directly.<sup>14</sup> The exclusion of cholesterol from DHA-rich regions in favor of interactions with saturated chains is also consistent with experimental and simulation reports on neat bilayers.<sup>20</sup>

Two important questions remain: Why are disk membranes so rich in cholesterol, and how can cholesterol stabilize rhodopsin in the absence of direct binding? To answer these questions, we have analyzed the transverse structure of the membrane by calculating the effective cross-sectional areas of the chemical components of the system as a function of distance from the membrane center; the results are shown as Figure 2. We computed these areas by selecting all atoms in 3 Å-thick slices from the system, projecting the atoms into a plane, and computing the Voronoi areas for each atom<sup>21</sup> (see Supporting Information for details). Two features immediately stand out: first, all of the components show significant asymmetry along the membrane normal, driven by the protein’s intrinsic asymmetry; second, the distribution of cholesterol areas complements that of rhodopsin. This suggests a mechanism by which the presence of cholesterol could stabilize the native state of rhodopsin even in the absence of direct protein–cholesterol interactions;<sup>7</sup> the cholesterol relieves the strain on the bilayer induced by rhodopsin’s hourglass shape. The results also suggest a mechanism for cholesterol’s experimentally observed inhibition of the photocycle;<sup>8,9</sup> when the protein conformation changes during the photocycle, altering its area profile, the natural complementarity between the protein and cholesterol areas may break down. If this is the case, cholesterol would selectively stabilize the native state, which would in turn slow the kinetics of the photocycle. Alternatively, the slowing could be the result of cholesterol’s stiffening effects on the membrane.<sup>22</sup> Interestingly, the overall distribution of cholesterol molecules observed here is similar to that found in

simulations of a neat cholesterol/SDPC bilayer,<sup>20</sup> suggesting that cholesterol has a naturally complimentary density distribution, i.e., the distribution does not have to shift from its free energy minimum to optimize packing in the retinal membrane.

Rhodopsin is important both biologically and as an exemplar for G-protein coupled receptors in general. Recent improvements in computer power and simulation techniques have made it possible to carry out detailed, atomic-level simulations of rhodopsin in a realistic membrane environment on relatively long time scales, paving the way for simulations of excitation and the photocycle. The present simulation has demonstrated the power of modeling studies to aid in the interpretation of experimental observations, such as the cholesterol-mediated recruitment of DHA by rhodopsin<sup>7</sup> and the dependence of rhodopsin activity on lipid type.<sup>8,9,23</sup>

**Acknowledgment.** We acknowledge the support of the Blue Matter Team (B. Fitch, R. Germain, A. Rayshubskiy, T. J. C. Ward, Y. Zhestkov, M. Eleftheriou, J. Pitera, and W. Swope). S.E.F. thanks the National Science Foundation for support through award MCB-0091508.

**Supporting Information Available:** Voronoi area computations, the distribution of the three hydrophobic bilayer components as a function of the signed distance to the protein surface, and details of system construction and simulation conditions. This material is available free of charge via the Internet at <http://pubs.acs.org>.

## References

- (1) Weiner, M. C.; White, S. *Biophys. J.* **1992**, *61*, 434–447.
- (2) Albert, A. D.; Young, J. E.; Yeagle, P. L. *Biochim Biophys Acta* **1996**, *1285*, 47–55.
- (3) Mitchell, D. C.; Straume, M.; Litman, B. J. *Biochemistry* **1992**, *31*, 662–670.
- (4) Stone, W. L.; Farnsworth, C. C.; Dratz, E. A. *Exp. Eye. Res.* **1979**, *28*, 387–397.
- (5) Boesze-Battaglia, K.; Hennessey, T.; Albert, A. D. *J. Biol. Chem.* **1989**, *264*, 8151–8155.
- (6) Feller, S. E.; Gawrisch, K.; Woolf, T. B. *J. Am. Chem. Soc.* **2003**, *125*, 4434–4435.
- (7) Polozova, A.; Litman, B. J. *Biophys. J.* **2000**, *79*, 2632–2643.
- (8) Mitchell, D. C.; Niu, S.-L.; Litman, B. J. *J. Biol. Chem.* **2001**, *276*, 42801–42806.
- (9) Niu, S.-L.; Mitchell, D. C.; Litman, B. J. *J. Biol. Chem.* **2001**, *276*, 42807–42811.
- (10) Huber, T.; Botelho, A. V.; Beyer, K.; Brown, M. F. *Biophys. J.* **2004**, *86*, 2078–2100.
- (11) Crozier, P. S.; Stevens, M. J.; Forrest, L. R.; Woolf, T. B. *J. Mol. Biol.* **2003**, *333*, 493–514.
- (12) Saam, J.; Tajkhorshid, E.; Hayashi, S.; Schulten, K. *Biophys. J.* **2002**, *83*, 3097–2112.
- (13) Rohrig, U. F., et al. *J. Am. Chem. Soc.* **2004**, *126*, 15328–15329.
- (14) Niu, S.-L.; Mitchell, D. C.; Litman, B. J. *J. Biol. Chem.* **2002**, *277*, 20139–20145.
- (15) Feller, S. E.; MacKerell, A. D., Jr. *J. Phys. Chem. B* **2000**, *104*, 7510–7515.
- (16) Feller, S. E.; Yin, D.; Pastor, R. W.; MacKerell, A. D., Jr. *Biophys. J.* **1997**, *73*, 2269–2279.
- (17) MacKerell, A. D., Jr., Atomistic Models and Force Fields. In *Computational Biochemistry and Biophysics*; Watanabe, M., Ed.; Marcel Dekker: New York, 2001; pp 7–38.
- (18) Palczewski, K., et al. *Science* **2000**, *289*, 739–745.
- (19) Okada, T., et al. *Proc. Natl. Acad. Sci. U.S.A.* **2002**, *99*, 5982–5987.
- (20) Pitman, M.; Suits, F.; MacKerell, A. D., Jr.; Feller, S. E. *Biochemistry* **2004**, *43*, 15318–15328.
- (21) Barber, C. B.; Dobkin, D. P.; Huhdanpaa, H. T. *ACM Trans. Math. Software* **1996**, *22*, 469–483.
- (22) Endress, E., et al. *Biochemistry* **2002**, *41*, 13078–13086.
- (23) Brown, M. F. Influence of Nonlamellar-Forming Lipids on Rhodopsin. In *Lipid Polymorphism And Membrane Properties*; Vol. 44; 1997; pp 285–356.

JA042715Y